ISBN: 978-3-95450-230-1 ISSN: 2673-5350 doi:10.18429/JACoW-IBIC2021-WEPP24

PSB H^0-H^- MONITOR CALIBRATION AND COMMISSIONING

A. Navarro*, S. Bart, D. Belohrad, C. Bracco, E. Renner, F. Roncarolo, J. Tassan-Viol,
CERN, Geneva, Switzerland

Abstract

During the LHC Long Shutdown 2 (LS2), the H^- LINAC4 replaced the proton LINAC2 as Proton Synchrotron Booster (PSB) injector. In each of the four PSB rings, the injection region was upgraded to accommodate the necessary elements for a proper H^- charge exchange injection system. Four beam dumps (one per ring), installed downstream the stripping foil, prevent the unstripped H^- particles from being injected in the ring. The H^0 H^- monitors, consist of four titanium plates placed a few centimetres upstream of the dump, intercept partially stripped H^0 or not stripped H^- ions and allow a continuous monitoring of the stripping efficiency, providing an interlock signal to block the injection process in the case of severe degradation or breakage of the foil, which would heavily damage the dumps.

This contribution focuses on the commissioning and operation of these new systems. It describes the results from the calibration campaigns, performed by comparison to beam current transformer measurements during special periods with low intensity beams and no stripping foil, and during normal operation, when it was already possible to monitor stripping inefficiencies below 1% and compare different beams and stripping foil types.

INTRODUCTION

The LHC high luminosity programme (HL-LHC) [1] calls for the production and acceleration of brighter beams from the injectors [2]. During the Long Shutdown 2 (LS2) at CERN, the new LINAC4 accelerator [3] was connected to the Proton Synchrotron Booster (PSB). It provides a 160 MeV H^- particle beam. With respect to the LINAC2, the increase of injection energy from 50 to 160 MeV doubles the relativistic factor $\beta\gamma^2$ at PSB injection allowing the beam brightness to be doubled. The beam from LINAC4 consists of four individual pulses, separated by a 1 µs particle-free gap and a pulse length that depends on the number of turns injected per ring. The pulses are then distributed to the corresponding booster rings for injection.

To inject the H^- beam in the PSB, a new charge exchange injection system [4] was installed in each ring. This new system reduces injection losses which were unavoidable in the previously used multi-turn injection. Figure 1 shows a schematic representation of the new injection system which comprises a stripping foil, a set of four pulsed dipole magnets (BSW) [5] and four horizontal kickers (KSW) [6] (Not indicated in the picture).

The first magnet (BSW1) acts as a septum generating a high-field region for the circulating beam and a field-free region for the injected H^- beam. It is followed by 3 bumper magnets (BSW2-4) that help merging the injected beam with the circulating beam. The stripping foil (about 20 mm wide and 20 mm high) is made of carbon with a density around 200 µgcm^{-2}. It strips electrons from the incident H^- particles. The characteristics of the used stripping foil have been optimized to provide sufficient stripping efficiency (> 99%) while minimizing emittance blow-up. After the stripping foil, fully-stripped protons are injected into the circulating beam while the partially-stripped and unstripped ions are collected by a dedicated dump.

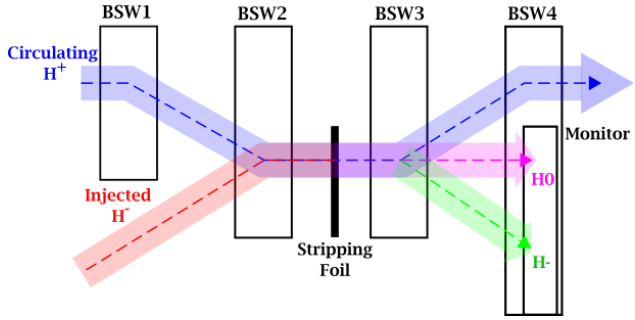

Figure 1: Schematic representation of PSB H- Charge injection system.

PSB H0H- BEAM CURRENT MONITOR

The injection region geometry and the very limited space available preclude extraction of the unstripped or partially stripped ions. For that reason, four internal Ti_6Al_4V dumps, one per ring, were installed downstream of the stripping foil, within the vacuum chamber of the chicane magnet BSW4, as shown in Figs. 2 and 3. The geometry of the dump provides an unobstructed passage for the circulating beam during injection as well as for the injected proton beam, whilst providing optimal protection of the downstream elements by absorbing a few percent of the unstripped beam during regular operation, and also by absorbing the full beam in the event of a foil failure. In Figs. 2 and 3 the dump is represented in black.

The H^0H^- monitors (represented in red in Figs. 2 and 3) are installed 4 cm upstream from the face of the dump. The dump is far enough from the detectors to prevent secondary electrons coming from the dump affecting the signal of the monitors. The H^0H^- monitors consist of four titanium plates: two 22 mm wide central plates and two 18 mm wide external plates with around 1 mm separation between the plates which allows to supplement the intensity measurements with some beam positioning information. The two outer plates are expected to measure H^- particles while

* araceli.navarro.fernandez@cern.ch

ISBN: 978-3-95450-230-1 ISSN: 2673-5350 doi:10.18429/JACoW-IBIC2021-WEPP24

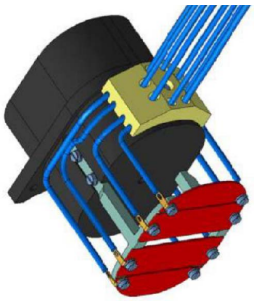

Figure 2: Mechanical design of the H^0H^- current monitors (red) and Ti_6Al_4V dump (black).

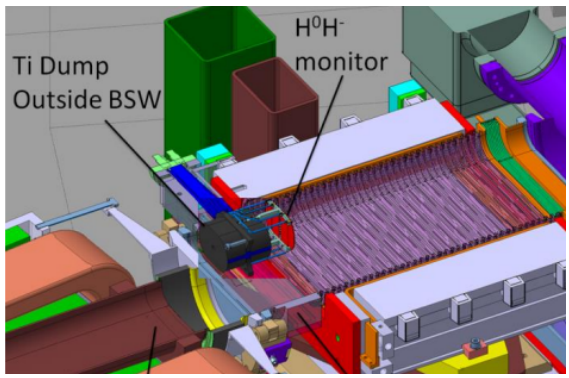

Figure 3: Integration of the H^0 H^- dump (black) and intensity monitor (red plates) in a PSB ring. The purple element is the BSW4 magnet.

the two inner plates are expected to measure the partially stripped H^0 particles.

The plates are made of titanium chosen for its low Z (i.e. low activation) and moderate conductivity ($2.34 \cdot 10^6\ \Omega^{-1}\mathrm{m}^{-1}$), which is a good compromise between the high conductivity needed for reading out the deposited charge and the low conductivity required due to the presence of a pulsed magnetic field in the BSW4 chamber. The thickness of 1 mm guarantees stopping all the stripped electrons and is compatible with the presence of a vertical B-field. No thermal problem is expected even if the stripping foil fails as the temperature at the center of the beam spot does not exceed 90 K.

As shown in Figs. 2 and 3, each monitor plate has two read-out cables (represented in blue). This duplication has been implemented only for hardware redundancy: in the case of cable damage, a second one will be immediately available. During operation only one signal cable per plate is connected to the acquisition system, as reading out both outputs simultaneously would heavily reduce the monitor's sensitivity.

EXPECTED SIGNALS

The electrical signal generated in the plates allows determining the number of H^0 and H^- particles reaching the dump, and thus the stripping inefficiency. Several effects contribute to the charge formation in the plates. The most relevant ones are charge deposition (Q_{dep}) and Secondary Emission (SE) charge generation (Q_{SE}):

$$Q\left(\frac{e}{Proj}\right) = Q_{dep} + Q_{SE} \tag{1}$$

For an accelerated ion with N_p protons in the nucleus and N_e electrons we can estimate the deposited charge as:

$$Q_{dep} = N_p \cdot \eta - N_e \cdot \mu \tag{2}$$

where η and μ represent the ratios of protons and electrons that remain in the material. In our particular case (160 MeV H^0 or H^- particles, 1 mm thick titanium plate) the values of these parameters were calculated using Geant4 10.07 as $\eta \approx 0.003$ and $\mu \approx 0.463$.

The SE charge (Q_{SE}) is generated when a particle passes through the interfaces of a material. The particle transfers energy to the electrons in the medium and if this energy is high enough they can escape the material. Such an emission process is known as Secondary Electron Emission (SEE) [7]. The main parameter describing the SEE is the Secondary Emission Yield (SEY) which is the average number of electrons emitted when an incident projectile enters or exits a surface. Q_{SE} can be estimated as:

$$\begin{aligned} Q_{SE} = 2 \cdot \left(N_p \cdot \eta \cdot SEY_p + N_e \cdot \mu \cdot SEY_e\right) \\ BS_p \cdot SEY_p + BS_e \cdot SEY_e \end{aligned} \tag{3}$$

where BS_e and BS_p are the ratios of backscattered particles with the indices p and e indicating protons and electrons, respectively. Their values were also calculated with Geant4 and in our particular case yield $BS_p \approx 0$ and $BS_p \approx 0.5369$. Table 1 presents the expected signals per an incident H^0 and H^- particle. The SE reduces the current measured by the intensity monitors. With the small energy of the SE, the magnetic field of BSW4 is large enough to suppress the SE. Thus, the expected charge per incident particle does not comprise the Q_{SE} term.

Table 1: Expected Net Charges per Incident H^0 and H^- Particle for a Titanium Detector, 1 mm Thickness, with (w. SE) and without (w.o. SE) Secondary Emission

	w. SE	**w.o. SE**
$Q\left(e/H^0\right)$	-0.2169	-0.463
$Q\left(e/H^-\right)$	-0.375	-0.975

The number of H^0 and H^- particles depends on the stripping efficiency. In normal operational conditions, during injection, the expected ratio of H^0 particles should be $< 2\%$ of the entire Linac4 pulse. The total ratio of H^- particles is expected to be very low $\approx 10^{-4}\%$. Stripping foil degradation is tolerated until the beam dump load reaches a safety limit. Currents larger than 10% of the Linac4 beam pulse generate an interlock signal that stops the particle beam.

ISBN: 978-3-95450-230-1 ISSN: 2673-5350 doi:10.18429/JACoW-IBIC2021-WEPP24

MEASUREMENT PROCEDURE

The main goal of the measurements was to obtain a calibration factor (R_{tot}) which, independently of the intensity or type of beam, relates the signal in the plates to the total number of particles reaching the dump. Several tests were performed with different configurations. In order to obtain a calibration factor independent of the stripping foil, all tests were performed with an H^- particle beam. This also allowed us to reach all the plates in the different detectors by properly adjusting some correctors and magnets.

The electronics of the H^0 H^- monitors are designed for accurately measuring a maximum of 10 % of the Linac4 beam pulse. For obtaining a non-saturated signal during the measurements, the calibration factor was calculated with a LINAC4 beam of reduced intensity (I_{beam} < 4 mA). The final calibration factor is independent of the beam intensity measured in each ring with Beam Current Transformers (BCTs) placed before the injection bump. The calibration factors were calculated for all plates in the rings, by comparing the signal measured in the plates with the signal measured by the BCTs:

$$R_i \left[\frac{Charge}{ADCcounts} \right] = \frac{SignalBCT}{SignalPlate} \quad (4)$$

In the above formula, the index i refers to the name of the plate. For convenience we will use H_{00}, H_{01}, H_{M0}, and H_{M1} to refer to the four different plates.

CALIBRATION FACTOR RESULTS

Figure 4 shows analog signals (boosted by a fast amplifier) measured by the H^0H^- monitors in Ring 4, for a beam pulse length of around 500 ns. Different colors represent signals measured by different plates. The particle beam was fully focused on the the plate closest to the beam pipe center (H_{00}). The signal measured by the plate has a negative amplitude as it is generated by charge deposition (Q_{dep}). The red curve shows the so-called integrating windows. Plate signals are integrated when the integration signal is positive. The length of this window can be modified but during the measurements it was set to integrate 720 ns over a 1 µs period, which captures the full length of the beam pulse.

Figure 5 shows the signals registered by the H_{00} plate in Ring4 after the full chain of electronics (filtering, amplifications, digitalization) for different beam conditions. Each point corresponds to the integral of one beam pulse. For longer beam pulses a larger number of particles reach the plates leading to a higher output current. On the other hand, a larger number of turns injected in that PSB ring results in a current observed for a longer time. These integrated signals are the ones that the user constantly monitors. The calibration factor was thus calculated by comparing these integrated signals and the intensities measured by the closest downstream BCTs. This comparison is also subjected to a correction factor that accounts for tail/head beam effects, beam placement, etc.

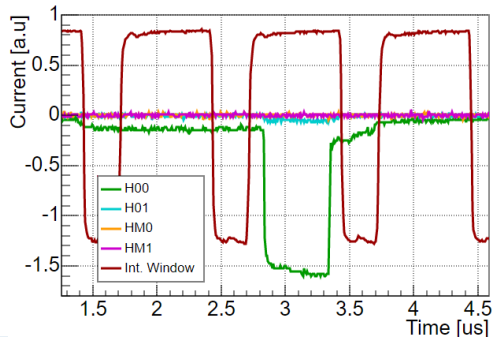

Figure 4: Signals from H^0H^- monitors in Ring4. Every color represents the signal generated in a different plate. The red curve shows the integration windows.

Figure 6 shows the calibration factors calculated for the H^0H^- intensity monitors in Ring1. One can distinguish two sets of points. The blue points were measured with BSW4 on i.e. when the H^0H^- intensity monitors were exposed to a constant magnetic field of around 0.18 T. Under such conditions, the obtained calibration factors were very similar for all the plates (R = $1.31(2) \cdot 10^{-8}$ [Charges/ADC count]). For the H_{00} and H_{01} plates, it was also possible to take measurements without the magnetic field (green points). In this case the calibration factor obtained was R = $1.67(2) \cdot 10^{-8}$ [Charges/ADC count]. The magnetic field of BSW4 is strong enough to suppress the low energy secondary electrons. This translates to an overall smaller signal measured in the plates and thus a higher calibration factor.

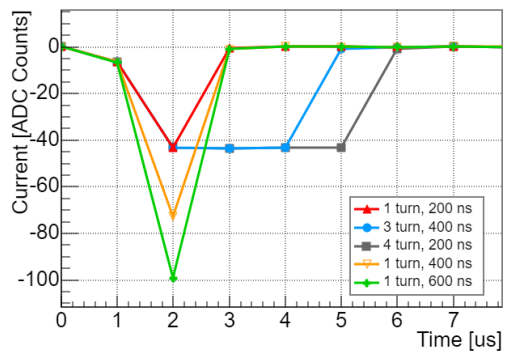

Figure 5: Signal of the H_{00} plate (Ring1) after the electronics chain, for several beam conditions.

Since during normal operation BSW4 remains turned on, the final value of the calibration factor was calculated in the presence of the BSW4 magnetic field. Figure 7 shows the calibration factors measured for all the plates, in all the PSB rings. The average calibration factor for all plates is R = $1.53 \cdot 10^{-8}$ [Charges/ADC counts] and it remains stable within 1.5 % for all plates under different beam conditions. Using this calibration factor, the total number of particles reaching the dump can be calculated as:

$$N_{Part} = R_{TOT} \cdot (2 \cdot H_{00} + 2 \cdot H_{01} + H_{M0} + H_{M1}) \quad (5)$$

ISBN: 978-3-95450-230-1 ISSN: 2673-5350 doi:10.18429/JACoW-IBIC2021-WEPP24

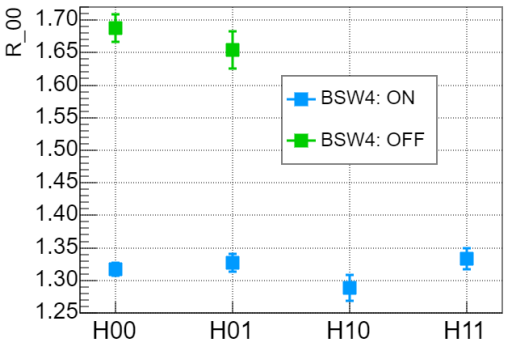

Figure 6: Calibration factor of the H0H- monitors in Ring 1, with BSW4 on and off. This factor is always measured in units of $10^{-8}[Charges/ADCCount]$.

where H_{00}, H_{01}, H_{M0}, and H_{M1} refer to the ADC counts measured by each plate. Doubling the H_{00} and H_{01} signal is necessary as during regular operation these plates are expected to measure uniquely H^0 particles. As it was previously shown, the net charge generated in H^0 is more or less half of what is generated in the H^- plates, due to H^0 only having one electrons. Nevertheless, the number of protons reaching the dump is the same in both cases.

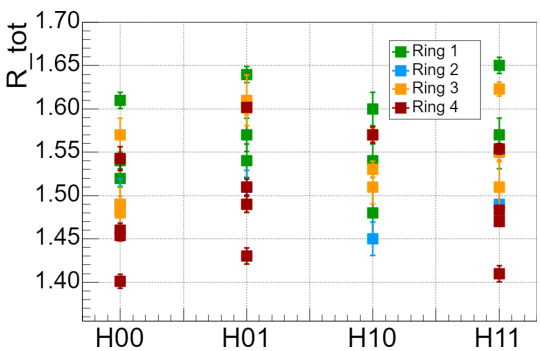

Figure 7: Calibration factors calculated for the different plates in the different rings, for different beam pulse lengths and number of turns. This factor is always measured in units of $10^{-8}[Charges/ADCCount]$.

STRIPPING INEFFICIENCY CALCULATIONS

Following the calibration phase, the H^0H^- monitors were used to measure the stripping efficiency from six different stripping foils (see Table 2 for their details). Figure 8 shows the distribution of the stripping inefficiency as measured by the H^0H^- monitors for this six foils. In all the cases, the measured stripping inefficiency was smaller than 1%.

CONCLUSIONS

During the Long Shutdown 2, LINAC4 replaced LINAC2 as PSB injector. The newly installed H^0H^- intensity monitors are indispensable for ensuring a proper charge exchange injection. They continuously measure the number of unstripped H^0 and H^- particles. The monitors are connected to an interlock system that blocks the injection process in the case of heavy degradation or breakage of the foil.

As presented in this paper, the H^0H^- intensity monitors have been fully commissioned. Due to the complexity of their electronics, a calibration factor was necessary to correlate the ADC signals with the number of particles reaching the dump. This factor was calculated by comparing the signals measured by the monitors and the closest upstream BCTs. A calibration factor R = $1.53{\cdot}10^{-8}$ [Charges/ADC Counts] was obtained. It remains stable within 1.5 % error for all plates in all PSB rings and for various beam conditions. It allows us to relate the signal provided by the monitors to the total number of particles reaching the dump.

The monitors are now in continuous operation to measure stripping inefficiencies smaller than 1% as well as to test stripping foils.

Table 2: Characteristics of the Measured Stripping Foils

Type	Weight	Description
XCF-200	200 µgcm^2	Arc evaporated amorphous Carbon
MLG-250	240 µgcm^2	Multilayer Graphene
GSI-200	200 µgcm^2	Arc evaporated amorphous Carbon

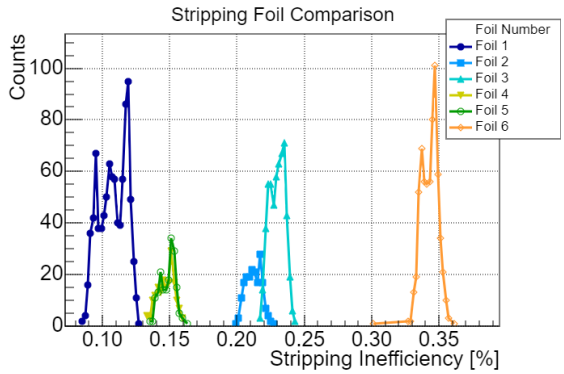

Figure 8: Stripping inefficiency as measured by the H^0H^- monitor in the PSB Ring 3 during dedicated studies with different foil types (preliminary results).

REFERENCES

[1] High Luminosity LHC Project, https://hilumilhc.web.cern.ch

[2] J. Coupard *et al.*, "LHC Injectors Upgrade, Technical Design Report, Vol. I: Protons", CERN, Geneva, Switzerland, Rep. CERN-ACC-2014-0337, 2014.

[3] L. Arnaudon *et al.*, "Linac4 Technical Design Report", CERN, Geneva, Switzerland, Rep. CERN-AB-2006-084, 2006.

[4] Dudnikov V G "Charge exchange injection into accelerators and storage rings", *Phys. Usp.*, vol 62, pp. 405–412, 2019.

[5] B. Balhan, C. Baud, C. C. M. Borburgh, and M. Hourican, "Design and Construction of the CERN PS Booster

ISBN: 978-3-95450-230-1 ISSN: 2673-5350 doi:10.18429/JACoW-IBIC2021-WEPP24

Charge Exchange Injection Chicane Bumpers", in *Proc. 9th Int. Particle Accelerator Conf. (IPAC'18)*, Vancouver, Canada, Apr.-May 2018, pp. 2575–2577. doi:10.18429/JACoW-IPAC2018-WEPMF082

[6] L. M. C. Feliciano *et al*., "A New Hardware Design for PSB Kicker Magnets (KSW) for the 35 mm Transverse Painting in the Horizontal Plane", in *Proc. 6th Int. Particle Accelerator Conf. (IPAC'15)*, Richmond, VA, USA, May 2015, pp. 3890–3892. doi:10.18429/JACoW-IPAC2015-THPF086

[7] E. J. Sternglass, "Theory of Secondary Electron Emission by High-Speed Ions", *Phys. Rev.*, vol. 108, p. 1, 1957.